JCTC Journal of Chemical Theory and Computation

pubs.acs.org/JCTC Article

Novel Approach for Predicting Vertical Electron Attachment Energies in Bulk-Solvated Molecules

Matheus B. Kiataki,* Márcio T. do N. Varella,* Kaline Coutinho,* and Franck Rabilloud*

Cite This: J. Chem. Theory Comput. 2024, 20, 4893−4900 Read Online

ACCESS | Metrics & More | Article Recommendations | Supporting Information

ABSTRACT: When low-energy electrons interact with molecules, they can give rise to transient anion states commonly known as resonances. These states are formed through vertical electron attachment processes and have the potential to induce various forms of DNA lesions, including base damage, single- and double-strand breaks, cross-links, and clustered lesions that are challenging to repair. So far, most experimental and theoretical studies have investigated the formation of resonances of (bio)molecules in the gas phase or in microsolvated environments. Since cellular environments are mainly composed of water molecules, it is crucial to understand how bulk water affects the resonances of (bio)molecules. Given the existing gap in studies on resonances of bulk-solvated molecules, we propose a novel theoretical-computational approach to address this void. Our approach combines the multibasis-set (time-dependent-)density functional theory and self-consistent sequential quantum mechanics/molecular mechanics polarizable electrostatic embedding methods. We apply this combined methodology to predict the vertical electron attachment energies of 1-methyl-5-nitroimidazole (1M5NI), a well-known radiosensitizer model, in bulk water. In addition, we analyze the rapid mutual polarization between the resonances (both shape- and core-excited) of 1M5NI and the surrounding bulk water environment. For comparison, we also studied the isolated and microsolvated 1M5NI. Overall, while the polarization of the environment is clearly sensitive to the solute charge, causing a significant impact on the vertical electron affinity and consequently on the attachment electron energies, it does not have a significant impact on the excitation energies of the anion.

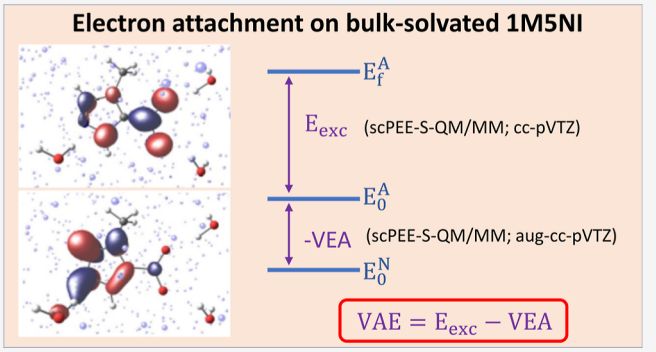

INTRODUCTION

Transient anion states formed by vertical electron attachment processes in biological environments are recognized for their potential to cause various types of DNA damage. These encompass base damage, single- and double-strand breaks, cross-links, and challenging-to-repair clustered lesions. The manifestation of these lesions stems from the decay of transient anion states, known as resonances, via dissociative electron attachment (DEA) or autoionization channels.[1−7] In DEA, a neutral radical and a stable anion are formed, while autoionization involves the detachment of the extra electron from the molecule. While the detrimental impact of DNA injuries induced by transient anions on healthy cells is unwelcome, their precise targeting at tumor tissues holds potential therapeutic benefits.[4,5,8] The idea of using the damage caused by transient anions to increase the effectiveness of radiation therapy is of great interest to the global scientific community. Numerous studies have explored potential radiosensitizing drugs to elucidate mechanisms associated with enhanced radiosensitivity, with the ultimate goal of applying these findings to the field of radiotherapy.[5,8−11]

Nitroimidazolic compounds constitute an important class of model radiosensitizers for the treatment of hypoxic tumors.[12] Experiments involving collisions of low-energy electrons with gaseous nitroimidazoles have demonstrated that these molecules undergo DEA.[13−19] It is widely believed that the radicals generated through DEA play a pivotal role in enhancing radiosensitivity. Recent experimental studies on the nimorazole[11] and metronidazole[18] molecules have additionally highlighted the formation of a nondecomposed free radical anion via the associative electron attachment process as a key factor in the radiosensitizing effect.

Although studies of nitroimidazoles and biomolecules in the gas phase have provided valuable insights, the role of water molecules prevalent in cellular environments cannot be ignored. Previous research has demonstrated that even a small number of water molecules can effectively inhibit DEA processes.[11,18,20−22] Furthermore, theoretical studies on molecules surrounded by a

Received: February 28, 2024
Revised: May 15, 2024
Accepted: May 15, 2024
Published: May 24, 2024

https://doi.org/10.1021/acs.jctc.4c00256
J. Chem. Theory Comput. 2024, 20, 4893−4900

few water molecules have indicated shifts in resonance energies.[23−31] The dependence of electron binding energies on the surrounding environment may result in the stabilization of anions in a solvent, whereas they are nonexistent or metastable in isolated species.[32] Also, dissociation and autoionization processes may not be the same when the anion is in bulk or in the gas phase as the radicals generated through DEA may interact with nearby molecules or the ejected electron can be captured by solvent molecules. To date, the effect of bulk solvation, prevalent in the cellular environment, on resonances remains poorly documented and understood.

Our study aims to address this gap by introducing a novel theoretical−computational methodology designed to predict vertical electron attachment energies (VAEs), commonly known as resonance energies, in bulk-solvated molecules. This methodology integrates standard electronic-structure methods, including density functional theory (DFT) and its time-dependent DFT (TDDFT) variant, with the self-consistent sequential quantum mechanics/molecular mechanics polarizable electrostatic embedding (scPEE-S-QM/MM)[33] method. Our primary objectives are 2-fold: (1) investigating the rapid mutual polarization between shape and core-excited resonances of bulk-solvated molecules and their surrounding aqueous environment; (2) predicting the resonance energies of bulk-solvated molecules. To exemplify our methodology, we focused on 1-methyl-5-nitroimidazole (1M5NI) in bulk water. This molecule, a well-known model radiosensitizer drug, has been extensively studied in the gas phase under exposure to incident electrons.[14,19,34,35] Significantly, 1M5NI shares structural similarities with nimorazole, a radiosensitizer drug employed in head and neck cancer treatments,[36] making it an intriguing system for in-depth investigation. Currently, a gap exists in our understanding of solvent effects on the resonance spectra of 1M5NI. Therefore, our work seeks to fill this void by predicting the resonance energies of 1M5NI in both bulk water and a microsolvated environment. Additionally, we calculated the resonance energies of the isolated 1M5NI for comparative analysis.

METHODS

Below, we outline the key components of the Monte Carlo (MC) simulations utilized for generating solute−solvent configurations, the combination of the multibasis-set (MBS) (TD-)DFT[37] and scPEE-S-QM/MM[33] methods, and the calculations of VAEs through this combined approach.

MC Simulations. The solute−solvent configurations composed of one 1M5NI molecule surrounded by 1000 water molecules were generated via MC simulations with the DICE software,[38] employing the isothermal−isobaric *NPT* ensemble at T = 298.15 K and P = 1 atm. Both the solute and solvent molecules were treated as rigid during the MC simulations, exploring only the translation−rotation configuration space. The ground-state geometry of 1M5NI was optimized with DFT, specifically employing the B3LYP exchange−correlation functional[39,40] and the aug-cc-pVDZ basis set within the Gaussian 09 program.[41] The optimal geometry in the gas phase was utilized for MC simulations as no significant disparities were observed compared to the optimal geometry obtained in an aqueous environment modeled by the polarizable continuum model (PCM).[42]

In the MC simulations, the intermolecular interactions were described with Lennard-Jones (LJ) and Coulomb potentials. The LJ parameters for the 1M5NI molecule were derived from the all-atom optimized potentials for liquid simulations (OPLS-AA).[43] The atomic charges of 1M5NI were calculated by fitting the QM electrostatic potential through the CHELPG method,[44] employing the second-order Møller−Plesset perturbation theory (MP2) and the aug-cc-pVDZ basis set. Additionally, in order to include the solute−solvent polarization in the MC simulations, the PCM model was used in the atomic charge calculation. Such an implicit polarization procedure has been successfully employed in previous studies.[45,46] Regarding water, we employed the geometrical and LJ parameters from the extended simple point charge (SPC/E) model.[47]

A total of 2.5×10^8 MC steps were run for the thermalization stage, followed by 2×10^9 MC steps for the production stage. Through the analysis of the solute−solvent hydrogen bonds (HBs), considering both energetic and geometrical criteria,[48,49] a subset of statistically uncorrelated MC configurations was selected to perform single-point calculations. We used $d_{DA} < 3.5$ Å [distance between the donor (D) and acceptor (A) atoms] and $\theta < 35°$ (angle among H-D-A atoms) as a geometrical criterion and $E_{int} < 0$ (interaction energy) as an energetic criterion.

Combination of the MBS (TD-)DFT and scPEE-S-QM/MM Methods. To predict the VAEs of bulk-solvated systems, we propose a combination of the MBS (TD-)DFT[37] and self-consistent sequential QM/MM polarizable electrostatic embedding (scPEE-S-QM/MM)[33] methods.

The MBS (TD-)DFT[37] method, hereafter referred to as MBS, has demonstrated the ability to accurately predict VAEs of systems in the gas phase by using the DFT and TDDFT methods along with the range-separated hybrid functional ωB97x[50] to compute, respectively, the vertical electron affinity (VEA) and electronic excitation energies (E_{exc}'s) of the anion. While a large basis set (e.g., aug-cc-pVTZ[51]) is used in the calculation of VEA, a small basis set, such as cc-pVTZ,[51] is employed to obtain the E_{exc}'s. The compact basis set prevents well-known intruder discretized continuum states in the spectrum of anion excited states and is suitable to describe valence excited states or localized states such as resonances. On the other hand, diffuse basis sets are important to provide an accurate VEA value. A given VAE of interest is then calculated by subtracting the anion electronic excitation energy and VEA, VAE = E_{exc} − VEA. This scheme has proved to be very efficient and reliable[52] as long as the anion does not undergo a dipole bound state.[53]

The scPEE-S-QM/MM[33] method is based on the sequential QM/MM approach[54,55] and is well-suited for polarizing the electrostatic embedding of solvent molecules. This is particularly beneficial when the electronic structure of the solute undergoes sudden changes, such as in vertical electronic excitation and vertical electron attachment or detachment processes. After solute−solvent configurations are generated via MC simulations, the polarization procedure for the electrostatic embedding environment begins. The procedure involves treating every molecule of the entire system (comprising solute and solvent molecules) individually at the QM level to recalculate its atomic charges under the influence of the electrostatic embedding formed by all other solvent and solute molecules. The solute molecule can be either in the ground or excited electronic state and in its neutral or charged forms. Initially, the SPC/E atomic charges are used for all solvent molecules, while the atomic charges for the solute in a given modified state of interest are obtained in the PCM environment. The atomic charges of each solvent molecule are then iteratively

https://doi.org/10.1021/acs.jctc.4c00256
J. Chem. Theory Comput. 2024, 20, 4893−4900

recomputed and updated several times until a convergence criterion is attained, thus completing a solvent polarization cycle. At the end of the cycle, the atomic charges of the solute are recomputed and updated in this new polarized electrostatic embedding environment, initiating a new polarization cycle for the solvent molecules. This iterative process continues until self-consistency is achieved between successive cycles. Through this iterative process of the scPEE-S-QM/MM method, both solute−solvent and solvent−solvent mutual polarizations are considered. We employ a convergence criterion of $\Delta\mu < 5 \times 10^{-4}$ D for the variation of the dipole moment of each solvent molecule and $\Delta q < 10^{-4}$ au for the variation of the atomic charges of each atom of the solute. The atomic charges of the solvent molecules and the solute in a modified electronic state were calculated by fitting the QM electrostatic potential with the CHELPG method[44] at the ωB97x/cc-pVTZ level. More comprehensive details of the scPEE-S-QM/MM method can be found elsewhere.[33]

Figure 1 shows the combined scheme for predicting VAEs of bulk-solvated systems. E_{exc} is computed with the cc-pVTZ basis

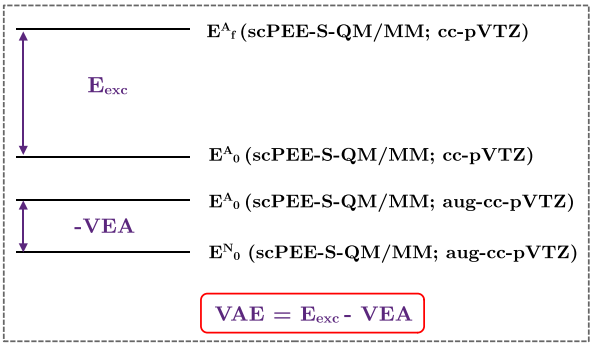

Figure 1. Depiction of the VAE computed with the combination of the MBS and scPEE-S-QM/MM methods. The VAE is calculated by subtracting the VEA from the anion excitation energy (E_{exc}). Within this combined approach, each electronic state of the solute in its anionic or neutral form is mutually polarized with the surrounding environment.

set, while the VEA is calculated using aug-cc-pVTZ. In the present study, the density functional ωB97x was employed in the calculation of both E_{exc}'s and VEA. To compute a given anion excitation energy, we subtract the ground-state energy (E_0^A) from the energy of the excited/final state (E_f^A), $E_{exc} = E_f^A - E_0^A$, whereas the VEA is calculated as the energy difference between the neutral and anion ground states, $VEA = E_0^N - E_0^A$. Each electronic state of the system in its neutral and anion forms is mutually polarized with its surrounding aqueous environment via the scPEE-S-QM/MM method. We considered the bulk-solvated neutral ground state (N) of 1M5NI and seven electronic anion states (A), namely, π_1^*, π_2^*, π_3^*, $n_-\pi_1^*$, $\pi_O\pi_1^*$, $\pi_1\pi_1^*$, and $n_+\pi_1^*$, where π_1^* is the bound anion ground state. The π_2^* and π_3^* states are shape resonances, while the other four states ($n_-\pi_1^*$, $\pi_O\pi_1^*$, $\pi_1\pi_1^*$, and $n_+\pi_1^*$) are core-excited resonances.

Although we have used here the TDDFT and DFT techniques with the aug-cc-pVTZ and cc-pVTZ basis sets, other electronic structure methods and basis sets could be employed to calculate electronic excitation energies and VEA within this combined method (MBS + scPEE-S-QM/MM).

Single-Point Calculations. From the MC simulations, we selected 30 statistically uncorrelated solute−solvent configurations to perform subsequent single-point calculations. These configurations involved three water molecules forming HBs with the 1M5NI solute, which, in turn, corresponds to the ensemble-averaged number of HBs in the presence of 500 additional water molecules. For each configuration, we calculated the energies of the virtual orbitals at the Hartree−Fock (HF)/6-31G(d) level for clusters composed of 1M5NI and three water molecules. According to Koopmans' theorem, the orbital energies provide estimates of the VAEs (resonance energies). From the distribution, we calculated the mean orbital energies. The cluster with the orbital energies closest to the mean values was designated as a representative cluster. Similarly, a representative configuration was selected based on the same procedure, now including the electrostatic embedding surrounding the clusters, i.e., the 500 water molecules described with SPC/E point charges in the calculations of the energies of the π^* virtual orbitals. Details on these approaches for choosing a representative cluster and configuration can be found elsewhere.[30,33]

With the representative configuration in hand, we combined both scPEE-S-QM/MM[33] and standard sequential QM/MM electrostatic embedding (EE-S-QM/MM) approaches with the MBS (TD-)DFT[37] method to predict the VAEs of the bulk-solvated 1M5NI. Unlike the scPEE-S-QM/MM method that generates individual polarized atomic charges for the solvent molecules, the standard EE-S-QM/MM approach uses static atomic charges of force fields, such as the SPC/E parameterization used here. The VAEs of the representative cluster, which correspond to microsolvated 1M5NI, were also computed. Additionally, to investigate the solvent influence on the VAEs, as well as on the VEA and anion excitation energies that contribute to the VAEs within the MBS scheme, we calculated the VAEs for isolated 1M5NI with both MBS and the stabilization method (SM).[56−58] To assess the quality of our results for bulk-solvated 1M5NI obtained from 3 QM water molecules plus 500 water molecules described with scPEE-S-QM/MM polarized atomic charges, we systematically increased the number of water molecules in the QM region and computed the VEA with the ωB97x functional but now employ the cc-pVTZ basis set instead of its augmented version to make these calculations computationally feasible.

RESULTS AND DISCUSSION

Figure 2 displays the solute−solvent minimum distance distribution function (MDDF), which describes the average distribution of solvent molecules around 1M5NI. In this distribution, three distinct structures are evident, corresponding to microsolvation, the first solvation shell, and the second solvation shell. By integrating the MDDF, we determined the occurrence of 3, 30, and 109 solvent molecules in the micro, first, and second solvation shells, respectively.

The converged dipole moments for each of the 500 water molecules surrounding the $[1M5NI\text{-}(H_2O)_3]^-$ cluster in its different electronic states are shown in Figure 3 (top panel). For any water−solute distance, the dipole moment value of the water molecules spreads considerably due to a local polarization effect, often exceeding the SPC/E value (2.35 D, horizontal line). This means that each water molecule is polarized by its local neighborhood. Of the 500 water molecules, ∼383 (77%) have dipole moment magnitudes greater than the SPC/E reference value of 2.35 D. For the remaining ∼117 solvent molecules (23%), the dipole moments are smaller than the SPC/E reference value. Notably, the polarization of water molecules is sensitive to anion states (shape or core-excited resonances) only

https://doi.org/10.1021/acs.jctc.4c00256
J. Chem. Theory Comput. 2024, 20, 4893−4900

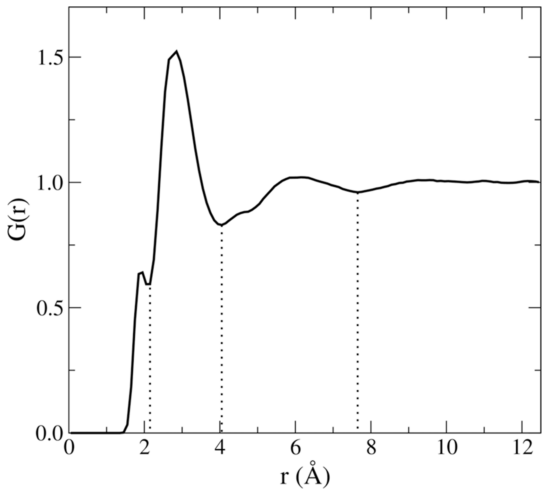

Figure 2. MDDF between the 1M5NI solute and water molecules. The solvation shells are indicated by the vertical dotted lines.

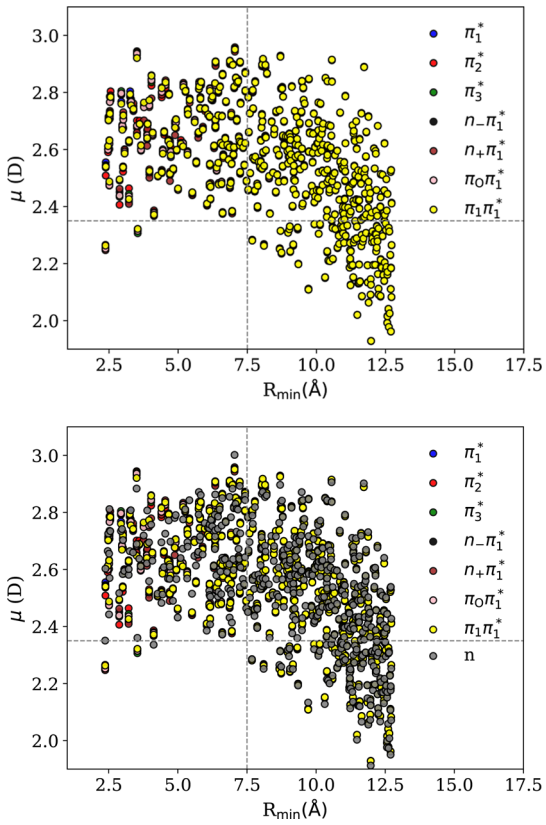

Figure 3. Converged dipole moments (μ) for the 500 water molecules of the aqueous environment polarized by different electronic states (π_1^*, π_2^*, π_3^*, $n_-\pi_1^*$, $n_+\pi_1^*$, $\pi_O\pi_1^*$, and $\pi_1\pi_1^*$) of the $[1M5NI\text{-}(H_2O)_3]^-$ cluster (upper panel) and also by the ground electronic state of the neutral cluster (n), 1M5NI-$(H_2O)_3$, (bottom panel). The dipole moment is shown as a function of the minimum distance to the solute (R_{min}). The horizontal lines correspond to the SPC/E value, while the vertical line (7.5 Å) indicates the onset of the vacuum effect (an artifact arising from the finite size of the system). The colored circles are plotted, state by state, in the order π_1^*, π_2^*, π_3^*, $n_-\pi_1^*$, $n_+\pi_1^*$, $\pi_O\pi_1^*$, and $\pi_1\pi_1^*$. Hence, some circles with different colors may be superimposed, e.g., the yellow circles in the top panel hide the other states when the value of μ does not significantly change with the electronic state of the $[1M5NI\text{-}(H_2O)_3]^-$ cluster.

within and around the first solvation shell, which extends up to ~4.0 Å. For larger distances, the water molecules cannot distinguish the anion's electronic states. The drop in dipole moment magnitude for some water molecules lying far from the solute, beyond 7.5 Å (vertical line), is a consequence of the vacuum effect, which was discussed in ref 33. This artifact stems from the finite size of the system considered in the calculations. In VAE calculations, we assigned the SPC/E atomic charges for water molecules that suffer from the vacuum effect. While state-sensitive polarization was observed only within and around the first solvation shell, charge-sensitive polarization was found for longer solute−solvent distances (see the bottom panel of Figure 3). Thus, even far-lying water molecules are affected by the solute charge, in consistency with our previous study.[33]

After understanding how different anion states (shape and core-excited resonances) as well as the ground electronic state of neutral 1M5NI-$(H_2O)_3$ polarize the surrounding watery environment composed of 500 water molecules, we now explore how the VAEs are affected by the aqueous medium described with the SPC/E (EE-S-QM/MM) and polarized point charges (scPEE-S-QM/MM). The predicted VAEs of bulk-solvated 1M5NI are shown in Table 1, along with the results obtained in the gas phase and the microsolvation environment. Results from other studies[34,35] are also included for comparison. Details of our results obtained with the SM can be seen in Figure 4, while the character of the anion states in bulk water is shown in Table 1 and also as Supporting Information.

Starting from the gas-phase VAEs in Table 1, there is good agreement between our MBS and SM estimates. The present results are also consistent with the experimental data[35] and other calculations.[34,35] Notably, the most significant discrepancy, approximately 0.4 eV, was found for the π_1^* ground anion state obtained at the MRCI/CCSDT(T) level,[35] which in turn corresponds to the −VEA (negative VEA). Besides, while the $\pi_O(\pi_1^*)^2$ and $\pi_1(\pi_1^*)^2$ anion states had a clearly different character in the MRCI/CCSD(T) study,[35] they became mixed in our MBS calculations (see Supporting Information). Under microsolvation, the VAEs are stabilized by ~0.7−1.0 eV with respect to the gas phase, thus showing the significant impact caused by the three H-bonded water molecules. The two anion states located at 2.86 and 3.09 eV involve transitions to the π_1^* orbital from similar occupied orbitals of π_O/π_1 mixed character (see the orbitals in the Supporting Information). When bulk solvation is described with the EE-S-QM/MM model, the VAEs exhibit less stabilization relative to the gas phase than the results obtained with microsolvation. In fact, the VAEs computed with the EE-S-QM/MM and microsolvation models are quite similar, with discrepancies ≤0.3 eV. If the electrostatic embedding is polarized with the scPEE-S-QM/MM model, a strong stabilization of the VAEs with respect to the gas-phase values is observed, around 1.3−1.7 eV. The importance of the environment polarization to the electron attachment is evident from the comparison between the EE-S-QM/MM and scPEE-S-QM/MM models. In general, the scPEE-S-QM/MM results show a stabilization of approximately 0.7−0.8 eV compared with the EE-S-QM/MM results.

Interestingly, the electronic excitation energies of the anion are less impacted by the presence of water molecules (Table 1). From the gas phase to the microsolvated case, the excitation energies are destabilized by 0.11−0.25 eV, and under bulk solvation effects, the destabilization relative to the gas-phase values is of 0.15−0.34 eV (EE-S-QM/MM) and 0.14−0.37 eV

https://doi.org/10.1021/acs.jctc.4c00256
J. Chem. Theory Comput. 2024, 20, 4893−4900

Table 1. VAEs of 1M5NI in the Gas Phase and in Microsolvated (Micro Results) and Bulk-Solvated Environments (EE-S-QM/MM and scPEE-S-QM/MM Results)[a]

		gas phase				micro	EE-S-QM/MM	scPEE-S-QM/MM	cLR-PCM
anion state	exp.[35]	MRCI/CCSD(T)[35]	SMC[34]	SMC[35]	SM	MBS	MBS	MBS	MBS
π_1^*		−0.35	−0.79	−0.79	−0.71	−0.78	−1.76	−1.65	−2.45	−3.08
π_2^*	2.0 ± 0.1	1.85	1.86	1.97	2.03	2.07 (2.85)	1.22 (2.98)	1.52 (3.17)	0.73 (3.18)	0.23 (3.31)
π_3^*	3.2 ± 0.1	3.12	2.93	3.22	2.95	3.04 (3.82)	2.17 (3.93)	2.32 (3.97)	1.51 (3.96)	1.01 (4.09)
$n_-\pi_1^*$	3.2 ± 0.1	3.55			3.49	3.43 (4.21)	2.58 (4.34)	2.78 (4.43)	1.99 (4.44)	1.32 (4.41)
$\pi_0\pi_1^*$	3.8−4.2	3.97			3.88	3.86 (4.64)	2.86 (4.62) | 3.09 (4.85)	3.25 (4.90)	2.45 (4.90)	1.91 (4.99)
$\pi_1\pi_1^*$	4.2−5.6	4.23			4.04	3.99 (4.77)	2.86 (4.62) | 3.09 (4.85)	3.04 (4.69)	2.26 (4.71)	1.67 (4.75)
$n_+\pi_1^*$	4.2−5.6	4.26			4.11	4.03 (4.81)	3.30 (5.06)	3.50 (5.15)	2.73 (5.18)	1.95 (5.03)

[a]Gas phase: isolated 1M5NI; micro: 1M5NI-$(H_2O)_3$; EE-S-QM/MM: 1M5NI-$(H_2O)_3$ + standard electrostatic embedding; scPEE-S-QM/MM: 1M5NI-$(H_2O)_3$ + polarized electrostatic embedding. The electronic excitation energies of the anion are indicated in parentheses. Experimental data[35] and other theoretical results[34,35] are also shown. MRCI, CCSD(T), SMC, and SM correspond, respectively, to the following methods: multireference configuration interaction, coupled cluster with singles and doubles plus perturbative triples, Schwinger multichannel method, and stabilization method. Calculation using the implicit solvation model cLR-PCM[59] is also given.

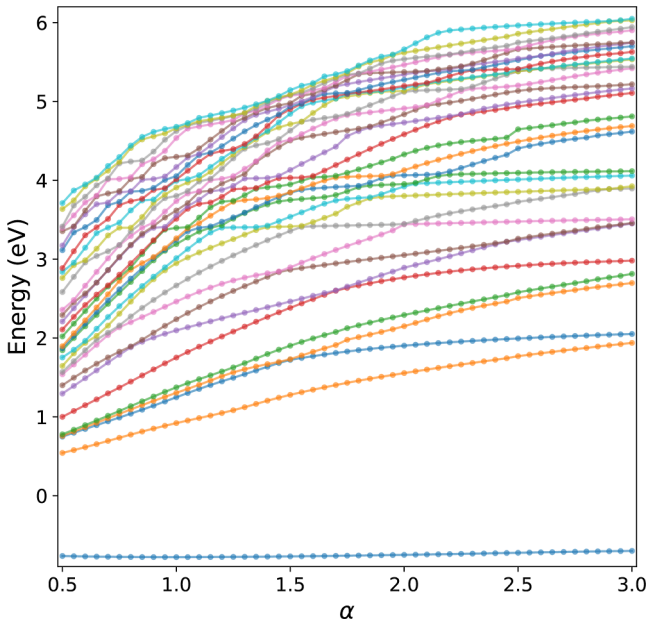

Figure 4. Stabilization graph for the electronic excitation energies of the isolated 1M5NI anion relative to the ground electronic state of the neutral. The most diffuse *s* and *p* functions were scaled by the α factor. The plateaus both above and below 0 eV correspond to the resonance energies and the binding energy of the anion, respectively.

(scPEE-S-QM/MM), although a subtle stabilization of 0.08 eV (EE-S-QM/MM) and 0.06 eV (scPEE-QM/MM) was found for the $\pi_1\pi_1^*$ anion state. Moreover, the polarization of the environment did not significantly impact the excitation energies of the anion (discrepancies ≤0.03 eV between the EE-S-QM/MM and scPEE-S-QM/MM results). This behavior is consistent with our previous discussion of the polarization of the aqueous environment by the different anion states (see Figure 3). Since most of the aqueous environment is insensitive to the different anion states, basically the same shifts are induced by the environment, thus preserving the anion excitation energies. On the other hand, the polarization of the environment is clearly sensitive to the solute charge, causing a significant impact on the VEA and consequently on the VAEs. These results shed light on the environmental effects on the VEA, electronic excitation energies, and VAE properties.

Interestingly, calculation using the implicit solvation model according to the corrected linear response PCM scheme (cLR-PCM[59]) is also given in Table 1. The VAEs computed with the implicit solvation model are about 0.5−0.7 eV lower than the scPEE-S-QM/MM values, while the excitation energies of the anion are somewhat similar. Implicit solvation models, while widely used, suffer from notable limitations, particularly in accurately representing site-to-site interactions, such as hydrogen bonding. The molecule 1M5NI, which forms an average of three HBs with surrounding water molecules, has its VEA and VAE properties significantly impacted by these water molecules. An explicit solvation model, such as scPEE-S-QM/MM, appears to be required.

To complete our analysis, we examined the quality of the results obtained with the minimal QM region composed of the solute and three H-bonded water molecules. For this purpose, the VEA was computed for increasingly large QM regions, i.e., by increasing the number of QM water molecules from the closest to the farthest, according to the MDDF. The results,

https://doi.org/10.1021/acs.jctc.4c00256
J. Chem. Theory Comput. 2024, 20, 4893−4900

shown in Figure 5, were calculated with the ωB97x functional but now with the nonaugmented basis, cc-pVTZ, for computational feasibility. The scPEE-S-QM/MM results show that the polarized atomic charges properly take into account solute−solvent and solvent−solvent mutual polarization effects in such a way that the expansion of the QM region size does not significantly affect the VEA. Only small fluctuations, ranging from 2.18 to 2.37 eV (orange area), are observed as the number of QM molecules varies from 3 to 203. Thus, the VEA is essentially converged with only 3 QM water molecules. Conversely, when the environment is not polarized according to the anion and neutral 1M5NI (EE-QM/MM results), the VEA value increases as the QM region is expanded (red area), although it is always underestimated, even with a considerably large number of QM water molecules (∼200).

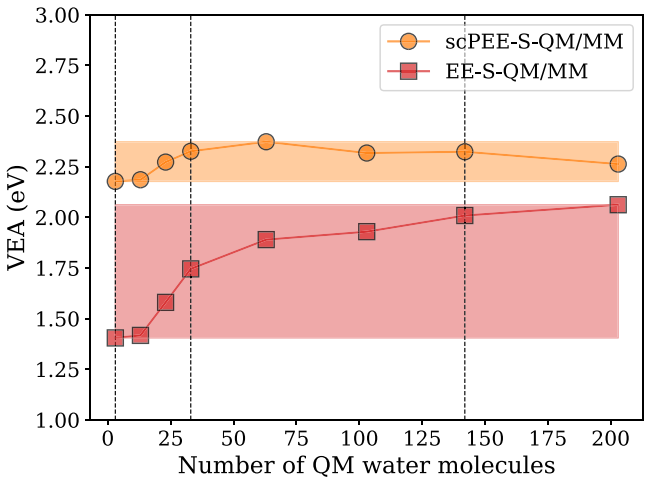

Figure 5. VEA as a function of the number of QM water molecules. These VEA results for different QM region sizes were obtained with the ωB97x functional and the cc-pVTZ basis set instead of its augmented version (aug-cc-pVTZ) to make the computational calculations viable. The EE-S-QM/MM model is a nonpolarized electrostatic embedding, which utilizes static SPC/E atomic charges to enclose the QM region. In contrast, the scPEE-S-QM/MM model is a polarized electrostatic embedding. Vertical lines indicate the accumulated number of water molecules up to the micro, first, and second solvation shells.

CONCLUSIONS

We propose a novel approach that combines the scPEE-S-QM/MM and the MBS (TD-)DFT methods to predict VAEs for bulk-solvated systems. This strategy enables us to comprehend in detail the fast mutual polarization between the shape and core-excited resonances of 1M5NI and its surrounding aqueous environment. Our results point out that the polarization of the watery environment is sensitive to the different electronic states of the anion only within and around the first solvation shell and sensitive to the solute's charge for all solute−solvent distances investigated. Since the VAE was decomposed into the electronic excitation energy of the anion and VEA, we investigated the influence of the solvent on these properties. While the anion excitation energies suffered a mild destabilization of 0.11−0.25 eV from the gas phase to the microsolvated condition, the VEA suffered a strong stabilization of ∼1 eV. As a result, the VAEs were significantly stabilized by 0.73−0.98 eV. From the microsolvation to the EE-S-QM/MM bulk solvation model, both excitation energy and VEA were slightly destabilized by 0.04−0.19 and ∼0.1 eV, respectively, thus causing a destabilization on the VAEs of ∼0.1−0.3 eV. However, when the fast response of the solvent to the vertical electron attachment process was taken into account through the scPEE-S-QM/MM method, the VEA was significantly stabilized by ∼0.7 eV in comparison to the microsolvation model, while the excitation energies were destabilized by ∼0.03−0.20 eV. As a result, the VAEs were stabilized by ∼0.5−0.7 eV relative to the microsolvated case.

Our results highlight the significant impact of charge-sensitive polarization of the aqueous environment on the VEA and consequently on the VAEs. Additionally, this study demonstrates that the anion excitation energies of bulk-solvated systems are barely affected by the electrostatic embedding model (polarized or not polarized) considered. In practical terms, excitation energies could be calculated using a simple nonpolarizable QM/MM approach, such as the standard electrostatic embedding (EE-S-QM/MM) explored here. However, for accurate values of VEA, we recommend using the scPEE-S-QM/MM method, which accounts for the solute−solvent and solvent−solvent mutual polarization effects.

Importantly, there is currently a lack of experimental or theoretical methods for predicting the resonance energies of bulk-solvated molecules. Our combined approach offers a valuable tool for estimating the resonance energies in bulk solvent scenarios, particularly for biomolecules and radiosensitizing drugs in bulk water. As the existing studies have primarily investigated the resonances of 1M5NI in the gas phase, our findings offer resonance values that better align with biological conditions. We aspire to this study to inspire researchers to conduct experiments and develop new theoretical methods capable of providing resonance data for bulk-solvated systems.

ASSOCIATED CONTENT

Supporting Information

The Supporting Information is available free of charge at https://pubs.acs.org/doi/10.1021/acs.jctc.4c00256.

Plots of the orbitals of the anion states of the isolated, microsolvated, and bulk-solvated 1M5NI (PDF)

AUTHOR INFORMATION

Corresponding Authors

Matheus B. Kiataki − *Universite Claude Bernard Lyon 1, CNRS, Institut Lumière Matière, UMR5306, Villeurbanne F-69100, France; Instituto de Física, Universidade de São Paulo, São Paulo 05508-090, São Paulo, Brazil;* orcid.org/0000-0002-3015-6212; Email: kiataki@usp.br

Márcio T. do N. Varella − *Instituto de Física, Universidade de São Paulo, São Paulo 05508-090, São Paulo, Brazil;* orcid.org/0000-0002-5812-0342; Email: mvarella@if.usp.br

Kaline Coutinho − *Instituto de Física, Universidade de São Paulo, São Paulo 05508-090, São Paulo, Brazil;* orcid.org/0000-0002-7586-3324; Email: kaline@if.usp.br

Franck Rabilloud − *Universite Claude Bernard Lyon 1, CNRS, Institut Lumière Matière, UMR5306, Villeurbanne F-69100, France;* orcid.org/0000-0002-5011-3949; Email: franck.rabilloud@univ-lyon1.fr

Complete contact information is available at: https://pubs.acs.org/10.1021/acs.jctc.4c00256

https://doi.org/10.1021/acs.jctc.4c00256
J. Chem. Theory Comput. 2024, 20, 4893−4900

Notes

The authors declare no competing financial interest.

■ ACKNOWLEDGMENTS

M.B.K. acknowledges financial support from CAPES-PRINT (grant no. 88887.694560/2022-00). M.T.d.N.V. also acknowledges financial support from CNPq (grant no. 304571/2018-0) and FAPESP (grant no. 2020/16155-7). K.C. acknowledges financial support from FAPESP (grant 2021/09016-3). F.R. acknowledges support from GENCI-IDRIS (grant A0150807662) and the Pôle Scientifique de Modélisation Numérique (PSMN).

■ REFERENCES

(1) Boudaïffa, B.; Cloutier, P.; Hunting, D.; Huels, M. A.; Sanche, L. Resonant Formation of DNA Strand Breaks by Low-Energy (3 to 20 eV) Electrons. *Science* **2000**, *287*, 1658−1660.

(2) Martin, F.; Burrow, P. D.; Cai, Z.; Cloutier, P.; Hunting, D.; Sanche, L. DNA Strand Breaks Induced by 0−4 eV Electrons: The Role of Shape Resonances. *Phys. Rev. Lett.* **2004**, *93*, 068101.

(3) Alizadeh, E.; Sanche, L. Precursors of Solvated Electrons in Radiobiological Physics and Chemistry. *Chem. Rev.* **2012**, *112*, 5578−5602.

(4) Alizadeh, E.; Orlando, T. M.; Sanche, L. Biomolecular Damage Induced by Ionizing Radiation: The Direct and Indirect Effects of Low-Energy Electrons on DNA. *Annu. Rev. Phys. Chem.* **2015**, *66*, 379−398.

(5) Rezaee, M.; Hill, R. P.; Jaffray, D. A. The Exploitation of Low-Energy Electrons in Cancer Treatment. *Radiat. Res.* **2017**, *188*, 123−143.

(6) Shao, Y.; Dong, Y.; Hunting, D.; Zheng, Y.; Sanche, L. Unified Mechanism for the Generation of Isolated and Clustered DNA Damages by a Single Low Energy (5−10 eV) Electron. *J. Phys. Chem. C* **2017**, *121*, 2466−2472.

(7) Dong, Y.; Gao, Y.; Liu, W.; Gao, T.; Zheng, Y.; Sanche, L. Clustered DNA Damage Induced by 2−20 eV Electrons and Transient Anions: General Mechanism and Correlation to Cell Death. *J. Phys. Chem. Lett.* **2019**, *10*, 2985−2990.

(8) Schürmann, R.; Vogel, S.; Ebel, K.; Bald, I. The Physico-Chemical Basis of DNA Radiosensitization: Implications for Cancer Radiation Therapy. *Chem.—Eur. J.* **2018**, *24*, 10271−10279.

(9) Sanche, L. Interaction of low energy electrons with DNA: Applications to cancer radiation therapy. *Radiat. Phys. Chem.* **2016**, *128*, 36−43. Radiation Physics and Chemistry of Biomolecules. Recent developments

(10) Gorfinkiel, J. D.; Ptasinska, S. Electron scattering from molecules and molecular aggregates of biological relevance. *J. Phys. B: At., Mol. Opt. Phys.* **2017**, *50*, 182001.

(11) Meißner, R.; Kočišek, J.; Feketeová, L.; Fedor, J.; Fárník, M.; Limão-Vieira, P.; Illenberger, E.; Denifl, S. Low-energy electrons transform the nimorazole molecule into a radiosensitiser. *Nat. Commun.* **2019**, *10*, 2388.

(12) Wardman, P. Chemical Radiosensitizers for Use in Radiotherapy. *Clin. Oncol.* **2007**, *19*, 397−417. Importance of Radiobiology to Cancer Therapy: Current Practice and Future Perspectives

(13) Tanzer, K.; Feketeová, L.; Puschnigg, B.; Scheier, P.; Illenberger, E.; Denifl, S. Reactions in Nitroimidazole Triggered by Low-Energy (0−2 eV) Electrons: Methylation at N1-H Completely Blocks Reactivity. *Angew. Chem., Int. Ed.* **2014**, *53*, 12240−12243.

(14) Tanzer, K.; Feketeová, L.; Puschnigg, B.; Scheier, P.; Illenberger, E.; Denifl, S. Reactions in Nitroimidazole and Methylnitroimidazole Triggered by Low-Energy (0−8 eV) Electrons. *J. Phys. Chem. A* **2015**, *119*, 6668−6675.

(15) Ribar, A.; Fink, K.; Probst, M.; Huber, S. E.; Feketeová, L.; Denifl, S. Isomer Selectivity in Low-Energy Electron Attachment to Nitroimidazoles. *Chem.—Eur. J.* **2017**, *23*, 12892−12899.

(16) Meißner, R.; Feketeová, L.; Illenberger, E.; Denifl, S. Reactions in the Radiosensitizer Misonidazole Induced by Low-Energy (0−10 eV) Electrons. *Int. J. Mol. Sci.* **2019**, *20*, 3496.

(17) Meißner, R.; Feketeová, L.; Bayer, A.; Limão-Vieira, P.; Denifl, S. Formation of negative and positive ions in the radiosensitizer nimorazole upon low-energy electron collisions. *J. Chem. Phys.* **2021**, *154*, 074306.

(18) Lochmann, C.; Luxford, T. F. M.; Makurat, S.; Pysanenko, A.; Kočišek, J.; Rak, J.; Denifl, S. Low-Energy Electron Induced Reactions in Metronidazole at Different Solvation Conditions. *Pharmaceuticals* **2022**, *15*, 701.

(19) Lozano, A. I.; Álvarez, L.; García-Abenza, A.; Guerra, C.; Kossoski, F.; Rosado, J.; Blanco, F.; Oller, J. C.; Hasan, M.; Centurion, M.; et al. Electron Scattering from 1-Methyl-5-Nitroimidazole: Cross-Sections for Modeling Electron Transport through Potential Radiosensitizers. *Int. J. Mol. Sci.* **2023**, *24*, 12182.

(20) Kočišek, J.; Pysanenko, A.; Fárník, M.; Fedor, J. Microhydration Prevents Fragmentation of Uracil and Thymine by Low-Energy Electrons. *J. Phys. Chem. Lett.* **2016**, *7*, 3401−3405.

(21) Poštulka, J.; Slavíček, P.; Fedor, J.; Fárník, M.; Kočišek, J. Energy Transfer in Microhydrated Uracil, 5-Fluorouracil, and 5-Bromouracil. *J. Phys. Chem. B* **2017**, *121*, 8965−8974.

(22) Ončák, M.; Meißner, R.; Arthur-Baidoo, E.; Denifl, S.; Luxford, T. F. M.; Pysanenko, A.; Fárník, M.; Pinkas, J.; Kočišek, J. Ring Formation and Hydration Effects in Electron Attachment to Misonidazole. *Int. J. Mol. Sci.* **2019**, *20*, 4383.

(23) Freitas, T. C.; Lima, M. A. P.; Canuto, S.; Bettega, M. H. F. Electron collisions with the CH_2O-H_2O complex. *Phys. Rev. A* **2009**, *80*, 062710.

(24) Freitas, T. C.; Coutinho, K.; Varella, M. T. d. N.; Lima, M. A. P.; Canuto, S.; Bettega, M. H. F. Electron collisions with the HCOOH···(H_2O)n complexes (n = 1, 2) in liquid phase: The influence of microsolvation on the π^* resonance of formic acid. *J. Chem. Phys.* **2013**, *138*, 174307.

(25) de Oliveira, E. M.; Freitas, T. C.; Coutinho, K.; Varella, M. T. d. N.; Canuto, S.; Lima, M. A. P.; Bettega, M. H. F. Communication: Transient anion states of phenol...(H2O)n (n = 1, 2) complexes: Search for microsolvation signatures. *J. Chem. Phys.* **2014**, *141*, 051105.

(26) Sieradzka, A.; Gorfinkiel, J. D. Theoretical study of resonance formation in microhydrated molecules. I. Pyridine-$(H_2O)_n$, n = 1,2,3,5. *J. Chem. Phys.* **2017**, *147*, 034302.

(27) Sieradzka, A.; Gorfinkiel, J. D. Theoretical study of resonance formation in microhydrated molecules. II. Thymine-$(H_2O)_n$, n = 1,2,3,5. *J. Chem. Phys.* **2017**, *147*, 034303.

(28) Fabrikant, I. I. Electron attachment to molecules in a cluster environment: suppression and enhancement effects. *Eur. Phys. J. D* **2018**, *72*, 96.

(29) McAllister, M.; Kazemigazestane, N.; Henry, L. T.; Gu, B.; Fabrikant, I.; Tribello, G. A.; Kohanoff, J. Solvation Effects on Dissociative Electron Attachment to Thymine. *J. Phys. Chem. B* **2019**, *123*, 1537−1544.

(30) Cornetta, L. M.; Coutinho, K.; Varella, M. T. d. N. Solvent effects on the π^* shape resonances of uracil. *J. Chem. Phys.* **2020**, *152*, 084301.

(31) Gorfinkiel, J. D. Electron collisions with molecules and molecular clusters. *Eur. Phys. J. D* **2020**, *74*, 51.

(32) Simons, J. Molecular anions perspective. *J. Phys. Chem. A* **2023**, *127*, 3940−3957.

(33) Kiataki, M. B.; Varella, M.T.d.N.; Coutinho, K. New approach to instantaneous polarizable electrostatic embedding of the solvent. *J. Mol. Liq.* **2023**, *389*, 122861.

(34) Kossoski, F.; Varella, M. T. d. N. How does methylation suppress the electron-induced decomposition of 1-methyl-nitroimidazoles? *J. Chem. Phys.* **2017**, *147*, 164310.

(35) Lozano, A. I.; Kossoski, F.; Blanco, F.; Limão-Vieira, P.; Varella, M. T. d. N.; García, G.; García, G. Observation of Transient Anions That Do Not Decay through Dissociative Electron Attachment: New Pathways for Radiosensitization. *J. Phys. Chem. Lett.* **2022**, *13*, 7001−7008.

https://doi.org/10.1021/acs.jctc.4c00256
J. Chem. Theory Comput. 2024, 20, 4893−4900

(36) Henk, J. M.; Bishop, K.; Shepherd, S. F. Treatment of head and neck cancer with CHART and nimorazole: phase II study. *Radiother. Oncol.* **2003**, *66*, 65−70.
(37) Thiam, G.; Rabilloud, F. Multi-Basis-Set (TD-)DFT Methods for Predicting Electron Attachment Energies. *J. Phys. Chem. Lett.* **2021**, *12*, 9995−10001.
(38) Cezar, H. M.; Canuto, S.; Coutinho, K. Solvent effect on the syn/anti conformational stability: A comparison between conformational bias Monte Carlo and molecular dynamics methods. *Int. J. Quantum Chem.* **2019**, *119*, No. e25688.
(39) Becke, A. D. Density-functional thermochemistry. III. The role of exact exchange. *J. Chem. Phys.* **1993**, *98*, 5648−5652.
(40) Lee, C.; Yang, W.; Parr, R. G. Development of the Colle-Salvetti correlation-energy formula into a functional of the electron density. *Phys. Rev. B* **1988**, *37*, 785−789.
(41) Frisch, M. J.; Trucks, G. W.; Schlegel, H. B.; Scuseria, G. E.; Robb, M. A.; Cheeseman, J. R.; Scalmani, G.; Barone, V.; Petersson, G. A.; Nakatsuji, H.; et al. *Gaussian16*. Revision C.01; Gaussian Inc: Wallingford CT, 2016.
(42) Tomasi, J.; Mennucci, B.; Cammi, R. Quantum Mechanical Continuum Solvation Models. *Chem. Rev.* **2005**, *105*, 2999−3094.
(43) Dodda, L. S.; Cabeza de Vaca, I.; Tirado-Rives, J.; Jorgensen, W. L. LigParGen web server: an automatic OPLS-AA parameter generator for organic ligands. *Nucleic Acids Res.* **2017**, *45*, W331−W336.
(44) Breneman, C. M.; Wiberg, K. B. Determining atom-centered monopoles from molecular electrostatic potentials. The need for high sampling density in formamide conformational analysis. *J. Comput. Chem.* **1990**, *11*, 361−373.
(45) Manzoni, V.; Lyra, M. L.; Gester, R. M.; Coutinho, K.; Canuto, S. Study of the optical and magnetic properties of pyrimidine in water combining PCM and QM/MM methodologies. *Phys. Chem. Chem. Phys.* **2010**, *12*, 14023−14033.
(46) Vequi-Suplicy, C. C.; Coutinho, K.; Lamy, M. T. Electric dipole moments of the fluorescent probes Prodan and Laurdan: experimental and theoretical evaluations. *Biophys. Rev.* **2014**, *6*, 63−74.
(47) Berendsen, H. J. C.; Grigera, J. R.; Straatsma, T. P. The missing term in effective pair potentials. *J. Phys. Chem.* **1987**, *91*, 6269−6271.
(48) Damasceno, M. V. A.; Costa Cabral, B. J.; Coutinho, K. Structure and electronic properties of hydrated mesityl oxide: a sequential quantum mechanics/molecular mechanics approach. *Theor. Chem. Acc.* **2012**, *131*, 1214.
(49) Canuto, S.; Coutinho, K. From hydrogen bond to bulk: Solvation analysis of the n-π^* transition of formaldehyde in water. *Int. J. Quantum Chem.* **2000**, *77*, 192−198.
(50) Chai, J.-D.; Head-Gordon, M. Systematic optimization of long-range corrected hybrid density functionals. *J. Chem. Phys.* **2008**, *128*, 084106.
(51) Kendall, R. A.; Dunning, T. H.; Harrison, R. J. Electron affinities of the first-row atoms revisited. Systematic basis sets and wave functions. *J. Chem. Phys.* **1992**, *96*, 6796−6806.
(52) Abdoul-Carime, H.; Thiam, G.; Rabilloud, F.; Charlieux, F.; Kopyra, J. Chemistry in Acetonitrile−Water Films Induced by Slow (<15 eV) Electrons: Application to the Earth and Space Chemistry. *ACS Earth Space Chem.* **2022**, *6*, 1126−1132.
(53) Thiam, G.; Rabilloud, F. How accurately can DFT describe non-valence anions. *J. Chem. Theory Comput.* **2023**, *19*, 2842−2849.
(54) Coutinho, K.; Canuto, S. *Solvent Effects from a Sequential Monte Carlo—Quantum Mechanical Approach*; Löwdin, P.-O., Sabin, J. R., Zerner, M. C., Karwowski, J., Karelson, M., Eds.; *Advances in Quantum Chemistry*; Academic Press, 1997; Vol. *28*, pp 89−105
(55) Coutinho, K.; Canuto, S.; Zerner, M. C. A Monte Carlo-quantum mechanics study of the solvatochromic shifts of the lowest transition of benzene. *J. Chem. Phys.* **2000**, *112*, 9874−9880.
(56) Holøien, E.; Midtdal, J. New Investigation of the $^1S^e$ Autoionizing States of He and H^-. *J. Chem. Phys.* **1966**, *45*, 3897.
(57) Sommerfeld, T.; Weber, R. J. Empirical Correlation Methods for Temporary Anions. *J. Phys. Chem. A* **2011**, *115*, 6675−6682.
(58) Falcetta, M. F.; DiFalco, L. A.; Ackerman, D. S.; Barlow, J. C.; Jordan, K. D. Assessment of Various Electronic Structure Methods for Characterizing Temporary Anion States: Application to the Ground State Anions of N_2, C_2H_2, C_2H_4, and C_6H_6. *J. Phys. Chem. A* **2014**, *118*, 7489−7497.
(59) Caricato, M.; Mennucci, B.; Tomasi, J.; Ingrosso, F.; Cammi, R.; Corni, S.; Scalmani, G. Formation and relaxation of excited states in solution: A new time dependent polarizable continuum model based on time dependent density functional theory. *J. Chem. Phys.* **2006**, *124*, 124520.

https://doi.org/10.1021/acs.jctc.4c00256
J. Chem. Theory Comput. 2024, 20, 4893−4900